Koninklijk Nederlands
Meteorologisch Instituut
Ministerie van Infrastructuur en Milieu

Mean precipitation changes and coastal effects in the ENSEMBLES regional climate model simulations

Jisk Attema and Geert Lenderink

De Bilt, 2011 | KNMI publication ; WR 201103

Royal Netherlands
Meteorological Institute
Ministry of Infrastructure and the Environment

Mean precipitation changes and coastal effects in the ENSEMBLES regional climate model simulations

Version 1.0

Date June 7, 2011
Status FINAL

Colofon

Title	Mean precipitation changes and coastal effects in the ENSEMBLES regional climate model simulations
Authors	J.J. Attema – T +3130 220 6832 G. Lenderink – T +3130 220 6438 Wilhelminalaan 10, 3732 GK De Bilt

Table of contents

Summary

Climate change values in the KNMI'06 scenarios do not discriminate within the Netherlands; thus changes in mean precipitation (and similarly, the wet-day frequency, a precipitation extreme occurring once every 10 years, and also temperature changes) are the same for the whole of the Netherlands for each of the four scenarios, G, G+, W and W+. Spatial patterns seen in the climate in 2050 or 2100 are therefore entirely related to differences already present in the present-day climate. One main reason for providing spatially uniform change values is that the available model integrations at that time (mostly from the PRUDENCE project) had an insufficient resolution of 50 km to be able to determine whether climate change could be different within the Netherlands.

Recently, an ensemble of 19 regional climate integrations with an increased resolution of 25 km has become available through the ENSEMBLES project [Hewitt and Griggs (2004)]. These integrations are based on the A1B emission scenario and run up to 2100. In this report we analyze this model ensemble and focus on mean precipitation changes and the effect of the North Sea on differences in precipitation between coastal and inland areas in the Netherlands.

Consistent with the range of projected changes in the KNMI'06 scenarios, we find an increase of approximately 20% in average winter precipitation, and a similar decrease in summer. No clear signal was found for spring and autumn, although these seasons seem to become slightly wetter by about 5%. Except for winter, the natural year-to-year variability of precipitation shows little change. The variability in winter increases by 20%, which can be attributed to the increase in mean precipitation.

Differences between precipitation in the coastal area and inland (hereafter, the coastal effect) are measured in this report by the difference between the area mean precipitation in the coastal area less than 50 km from sea and the inland area further away. In an average sense, the regional model ensemble is reasonably able to reproduce the observed coastal effect for spring (-0.2 mm day^{-1}) and autumn (0.3 mm day^{-1}) in the current climate (1970-2000). The ensemble median is close to these observations. Yet, a considerable number of the model simulations, approximately 30-40%, deviate clearly from the observations. For winter and summer observed coastal effects are small. For these seasons the majority of models deviate strongly from the observations, and also the median of the model results is biased (toward +0.1 in winter and -0.2 mm day^{-1} in summer).

In the ENSEMBLES integrations there is a small tendency towards an increase in coastal effect during the 21st century, in particular for summer and winter. The ensemble median predicts increases of 0.06 mm day^{-1} in summer, 0.05 mm day^{-1} in winter, 0.02 mm day^{-1} in spring, and 0.01 mm day^{-1} in autumn by the end of this century. Despite that changes in coastal effect in the analysed ENSEMBLES simulations are small in absolute terms, they are moderately large in relative terms. Changes are approximately 20-30% of the observed coastal effect in the present-day climate, and therefore may not be negligible.

Two important limitations of the results are worth mentioning. The results are hampered by the still relative coarseness of the model data (25 km) and the lack of a high resolution prescription of the sea surface temperature (SST) of the North Sea. Due to the coarse resolution a rather broad coastal zone of 50 km had to be chosen.

With this measure, and on a seasonal time scale, the coastal effect is smoothened out considerably. Even in the observations of the present-day climate the coastal effect is only 10-15% of the total precipitation amount with this measure. On a monthly time scale and on a smaller spatial scale the coastal effect is much larger. For instance, in October precipitation amounts are 30-40% higher close to the coast than inland. SST changes of the North Sea are relatively small ($\sim$2-3 degrees by the end of this century) in the ENSEMBLES simulations. This is due to the fact that the regional models use the SST fields directly derived from the driving global circulation models, which do not contain realistic prescriptions of the North Sea basin. To conclude, higher resolution and a more realistic description of North Sea temperatures are required to improve our estimates of how coastal effects in precipitation may change in the future climate. Work on this is in progress.

1 Introduction

1.1 KNMI’06 scenarios

In 2006 KNMI presented a new set of four climate scenarios for the Netherlands. These KNMI’06 scenarios used information from global climate models running at a low resolution for the whole globe, and regional climate models running at higher resolution for Europe. Model results were combined with observations and rules based on physical understanding of the climate system to obtain the scenarios [van den Hurk et al. (2006); Lenderink et al. (2007)].

In the KNMI’06 climate scenarios only one single value for precipitation changes for the whole of the Netherlands is provided per scenario; that is, changes in mean precipitation, wet-day frequency, or the extreme occurring once every 10 years, are the same for the whole of the Netherlands in each of the four scenarios. Spatial differences within the Netherlands in the future climate (for example, around 2050) are therefore entirely related to the differences already apparent in the present-day climate, and are not related to climate change.

There are several reasons for the decision to provide only single change values for the whole of the Netherlands. One obvious reason is that the at-the-time available regional climate model (RCM) integrations had a rather low horizontal resolution of 50 km, which was state-of-the-art, but which was considered insufficient to discriminate within the Netherlands since coastal zones or e.g. Lake Yssel (het IJsselmeer) are hardly resolved at that resolution. Apart from that, there were insufficient regional climate model runs available to determine whether the simulated differences within the Netherlands, as seen in the simulations, were statistically significant or whether they occurred due to chance. Spatial patterns on a scale of 200-1000 km also differed considerably in the global climate model (GCM) simulations analyzed for the KNMI’06 scenario’s; see Figure 4.2 in van den Hurk et al. (2006). However, a considerable part of these spatial differences are likely due to natural internal variability of the climate system, and are not caused by climate change. Finally, with the construction of the KNMI’06 scenario, statistical techniques had to be applied to obtain a realistic uncertainty range from the regional climate model simulations in accordance with the global climate model simulations. These statistical techniques – mainly pooling data from larger areas – were at the expense of the horizontal resolution [Lenderink et al. (2007)].

1.2 Coastal effects

Differences in precipitation climatology are considerable over the Netherlands. Precipitation amounts are smaller in the coastal zone in spring and larger in (late) fall compared to inland zones (figure 1.1). The North Sea plays an important role in explaining these differences, which are primarily related to temperature (and humidity) contrasts between sea and land. In autumn, warm and wet air above the sea leads to convective showers, some of which rain out over the coastal region. This results in an increased amount of precipitation for coastal areas. The effect is opposite in spring. Cold and moist air which originates from the sea becomes unstable over the warmer land. Showers develop and rain out some distance from sea.

Rising North Sea surface temperatures could have a different impact on coastal and inland precipitation, and therefore change the precipitation distribution within the Netherlands. For the month August 2006 model simulations with the regional climate model RACMO2 at very high resolution showed that approximately 30% of the

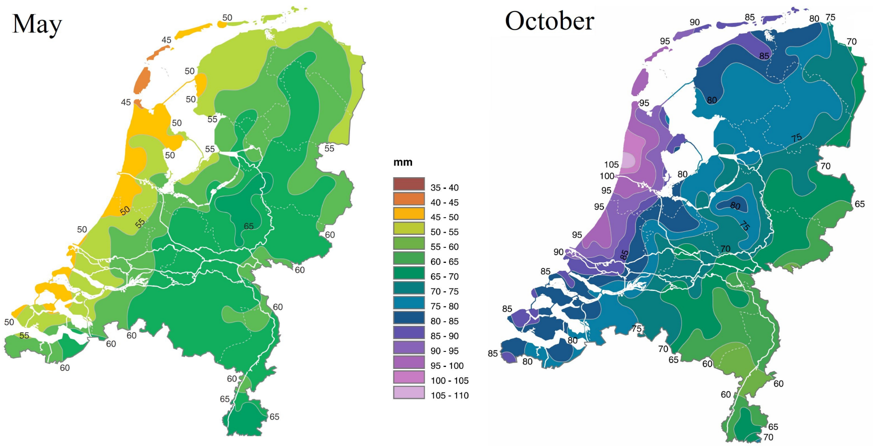

Figure 1.1: Observed average monthly precipitation for the period 1971-2000 for the months May and October, taken from the Klimaat Atlas.

precipitation in the coastal area was due to the anomalously high sea surface temperature (SST) of the North Sea [Lenderink et al. (2009)]. This was caused by a very warm spring and early summer until end of July in 2006, which led to North Sea temperatures more than 2 degrees above normal at the start of August. During the last 50 years the coastal area has also become wetter in summer compared to the inland area; see Lenderink et al. (2009) and this study.

How (and even whether) rising temperatures of the North Sea due to climate change could influence the precipitation distribution within the Netherlands in the future climate is, however, not well understood. One reason being that the present-day climatological distribution of precipitation is to a large extend caused by temperature differences between land and ocean, and these differences may not change much in the future. Further, dependencies of the coastal effect of precipitation on the sea surface temperature also strongly depend on the atmospheric conditions, such as the atmospheric flow. Strong dependencies occur when cold and unstable air is transported with a (north) westerly circulation over the land. It is not clear how these circulation statistics will change. Finally, a factor could be the availability of moisture at the end of the summer season. Many global and regional climate models project large scale drying out of the soil over the continents for the end of this century. Yet, the North Sea will obviously not dry out and the atmospheric moisture content over sea will increase at a rate close to 7% per degree following the Clausius-Clapeyron relation [Held and Soden (2006); O'Gorman and Muller (2010)]. Therefore, moisture contrasts between the continent and areas affected by the North Sea are expected to increase, and thus could enhance the coastal effect.

1.3 Regional climate model integrations

Recently, an ensemble of 19 regional climate runs with an increased resolution (25 km) has become available through the ENSEMBLES project [Hewitt and Griggs (2004)]. All of these model integration cover the full period 1950 to 2050, and most of the integrations extend until 2100. The model integrations use the A1B emission scenario, except one which uses the A2 scenario. Both A1B and A2 are moderately high emission scenarios. The ensemble predicts a 2 to 3 $^\circ$C increase in temperature by 2100 over the Netherlands. We note, however, that this increase is to a large extent imposed by the global climate model integrations that were used to force the regional model integrations. These global models have, with one exception, an average climate sensitivity – the climate sensitivity is the response of the global mean temperature to a doubling of greenhouse gas concentrations. Thus, this ensemble does not cover the upper and lower end of the projections of climate changes for Europe, but primarily represents "mainstream" scenarios.

The ensemble contains 19 regional model integrations, driven by the following global climate models: HadCM3Q16 (2), HadCM3Q3 (2),HadCM3Q0 (5), ECHAM5 (6), ARPEGE (2), CGCM3 (1), and BCM (1), with between curves the number of regional model integrations (see table 1.1). Regional climate model integrations driven by the same global model are indicated by the same symbol in the graphs. There are three versions of the global model HadCM3 involved: the standard version HadCM3Q0, and two versions with adapted physical parameterizations, one with a high climate sensitivity HadCM3Q16, and one with a low climate sensitivity HadCM3Q3. Different model integrations of ECHAM5 were available, but 5 out of the six regional model integrations use identical boundaries derived from ensemble member 3 (r3) of the ECHAM5 integrations using the A1B emission scenario. Thus, despite that 7 different global model versions provide boundaries in ENSEMBLES, 10 regional climate model integrations actually use boundaries from only two of these. In addition, the climate change signal, such as the global temperature response and the response in atmospheric circulation over Europe, is also quite similar in these two integrations. Therefore, it is important to realize that results of this ensemble are potentially biased and could under-sample the uncertainty range.

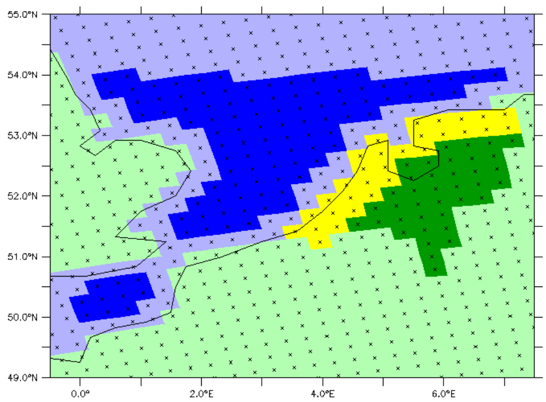

Figure 1.2: Regions used in the following analysis: the inland area (dark green), the coastal area (yellow), and the North Sea (dark blue). The total land area of the Netherlands is the sum of the green and yellow area. Grid points for model M11 (RACMO2) added.

The model domain of the regional climate runs covers an area from Iceland to Portugal and extends to roughly half-way the Black Sea. For the analysis we define three regions of interest: the inland area, the coastal area, and the North Sea. The coastal area is defined as the area in the Netherlands less than 50 km from the coastline, whereas the inland area is the area further away from the coast. A grid point is in the Netherlands if its center falls within the Netherlands as defined by a high-resolution border. This border is extended outwards by 5 km, so that also points that are just above sea are included into the coastal zone.

The North Sea is defined by all grid points between 0 by 8 East and 50 by 54 North that are "sea" according to the model's land-sea fraction (given by SFTLS in the

Model	Scenario	Global model	Regional model	Institute	Period	SST	Legend
M1	A1B	HadCM3Q16	HadRM3Q16	HC	150	No	
M2	A1B	HadCM3Q16	RCA3	C4I	150	Yes	
M3	A1B	HadCM3Q3	RCA	SMHI	150	Yes	
M4	A1B	HadCM3Q3	HadRM3Q3	HC	150	No	
M5	A1B	HadCM3Q0	CLM	ETHZ	150	Yes	
M6	A1B	HadCM3Q0	HadRM3Q0	HC	150	No	
M7	A1B	HadCM3Q0	HIRHAM	METNO	100	No	
M8	A1B	HadCM3Q0	PROMES	UCLM	100	Yes	
M9	A1B	HadCM3Q0	RRCM	VMGO	100	Yes	
M10	A1B	ECHAM5-r3	DMI-HIRHAM5	DMI	150	Yes	
M11	A1B	ECHAM5-r3	RACMO2	KNMI	150	Yes	
M12	A1B	ECHAM5-r3	REMO	MPI	150	Yes	
M13	A1B	ECHAM5-r3	RegCM	ICTP	150	Yes	
M14	A1B	ECHAM5-r3	RCA	SMHI	150	Yes	
M15	A2	ECHAM5	RCA3	C4I	100	Yes	
M16	A1B	ARPEGE	Aladin	CNRM	100	Yes	
M17	A1B	ARPEGE	HIRHAM	DMI	150	Yes	
M18	A1B	CGCM3	CRCM	OURANOS	100	Yes	
M19	A1B	BCM	RCA	SMHI	150	Yes	

Table 1.1: The members of the multi-model ensemble and the legend for most of the figures in this report.

ENSEMBLES data base) and that are at least 1 grid point removed from the coast (that is, all neighbours are sea). The last step was necessary to remove grid points with obviously erroneous SSTs in the output of some regional climate models (most likely caused by interpolation errors due to use of "land" values in the SST output field). In figure 1.2 the different regions are indicated for the KNMI regional climate model RACMO2. The regions contain 30 (coast), 38 (inland), and 98 (North Sea) grid points.

For comparison with observations three datasets are used. For precipitation we compare with the E-OBS data set [Haylock et al. (2008); eca.knmi.nl]; for the SSTs the OIv2 [Reynolds et al. (2002)] as well as an ERA40 [Uppala et al. (2005)] reanalysis are used.

In this report we analyse averages of the precipitation over the Netherlands and the effect of the North Sea on differences in precipitation between the coastal and inland areas. In the main text we only show limited information on the behavior of the separate models. Plots containing separate model results can be found in the Appendix.

2 Mean precipitation

2.1 Present-day climate

Results of the transient regional climate model integrations for the present-day climate (period 1970-1999) are compared to the E-OBS observational data base. For this purpose each model integration is attributed the same probability, and the resulting distribution of model outcomes is then compared to the observations. Figure 2.1 shows the mean precipitation over the Netherlands (coast plus inland regions from figure 1.2) in the model ensemble for the different seasons, winter (DJF), spring (MAM), summer (JJA) and autumn (SON).

All regional climate models have also been forced by realistic boundaries for the present-day climate derived from the ERA40 reanalysis [Uppala et al. (2005)]. These runs provide a well controlled benchmark of the quality of the regional climate models in the ENSEMBLES project [Hewitt and Griggs (2004)]. By comparing these results with those obtained with the GCM boundaries, we can separate errors in the RCM simulations due to errors in the boundary forcing from errors internally generated by the RCM. Therefore, we discus results from these ERA40 driven integrations together with those of the transient climate integrations.

The majority of the transient model integrations are too wet compared to E-OBS. One model, M9, displays very large biases of order +100%, for winter and spring far outside the range covered by the other models. Also other results of this model appear unreliable, and therefore we exclude this model in the following discussion in this and the next chapter. However, for completeness we retained the results from this model in the following figures (although sometimes the results are even outside the range plotted in the figures).

In winter all model integrations have a positive bias, and the median of the model integrations is almost 50% higher than E-OBS (3.0 mm day^{-1} compared to 2.1mm day^{-1}, respectively). Half of this bias, however, can be explained by the fact that the integrations are forced by runs from a global climate model which also contains errors in the lateral boundaries provided to the regional climate models. For instance, the overestimation of precipitation could be due to a too strong westerly flow in the driving GCM simulations. In runs driven by ERA40 derived boundaries precipitation amounts are typically 2.5 mm day^{-1}, closer to the E-OBS observations.

Spring shows similar results, yet with generally smaller values of the bias. Also the difference between the ERA40 and GCM driving simulations is now rather small.

In summer and, in particular, in autumn the range in simulated precipitation is large, and the simulated seasonal mean precipitation differs a factor two between the models contained in the ensemble. The same models driven by ERA40 boundaries, however, show much smaller variations. The correspondence with the observations in these ERA40 driven integrations is similar to the results for winter and spring, and therefore the quality of the GCM boundaries appear to be the main reason for the large spread in the GCM driven simulations.

That the driving global model determines most of the behaviour is confirmed by considering model integrations that have been driven by HadCM3Q0 (that is, M5 through M8, M9 excluding as mentioned above) and ECHAM5r3 (M10 through M14). We note that M15 is also using an integration from the same model ECHAM5. For summer and autumn all ECHAM5 driven integrations are in the top half of the

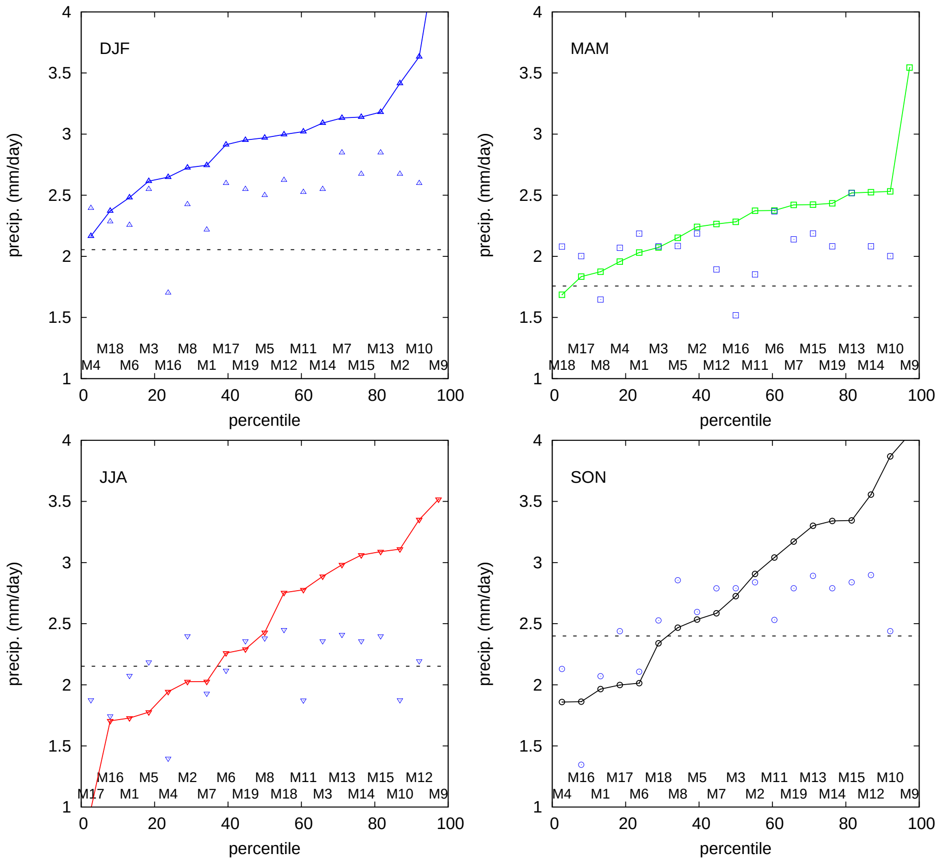

Figure 2.1: Mean precipitation averaged over the Netherlands for the period 1970-1999 in the model ensemble. The distribution of the 19 model results driven by the GCM boundaries is plotted as a percentile plot (connecting symbols) with Mxx referring to the corresponding regional model simulation as given in table 1.1. The ERA40 driven results are shown by the unconnected symbols, the dotted lines indicate observations from E-OBS.

distribution, whereas results from HadCM3Q0 display lower precipitation amounts which are closer to the E-OBS data.

Looking at the individual models a few results are worth mentioning. HIRHAM (M10) shows very large differences between the ECHAM5-r3 driven transient integration and the ERA40 integration; the ERA40 driven integration has small biases whereas results of the transient integration is far from the observations. Compared to the other ECHAM5-r3 driven simulations, this difference is much larger for summer and autumn. This is unusual because it is commonly believed that, besides the summer season, mean precipitation amounts are primarily set by the lateral boundary conditions. Therefore, this could point at a possible problem with this integration. The ERA40 simulation of M16 is too dry for all seasons, in particular for autumn. The KNMI regional climate model (M11) shows good results for spring and autumn when forced by ERA40 boundaries, but the simulation is too wet in winter and too dry in summer. We note that the observations may be biased too, in particular in the winter season, since E-OBS does not explicitly correct for under-catchment due to the wind.

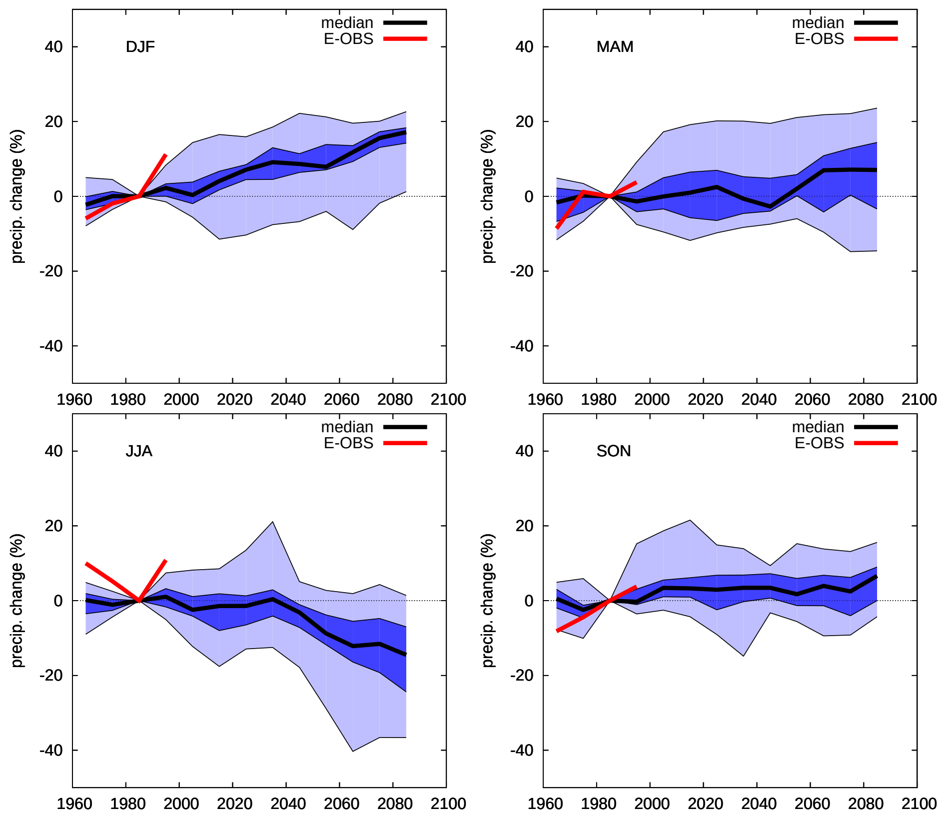

Figure 2.2: Trends in the average precipitation over the Netherlands relative to the control period 1970-1999. Shown are the median of the response in the model ensemble, the 25th to 75th percentile range (dark blue shading), and the full spread in the model ensemble (light blue shading) of a 30-year period moving with steps of 10 years. Also shown is the trend derived from E-OBS (red line).

2.2 Climate change

In figure 2.2 we show the trend in precipitation over the Netherlands (average of coast and land regions from figure 1.2). We calculated 30-year averages with the 30-year window moving in steps of 10 years. Results are show as a relative change with respect to the 1970-2000 mean. Plotted are the ensemble median and the range covering middle 50% (dark blue) and 100% (light blue) of the ensemble members. We note that six model integrations only ran up to 2050. To retain as much data as possible we kept the results of these models, but we note that this sometimes results in a discontinuity at 2035 (period 2020-2050). The following trends in mean precipitation can be seen.

In winter an almost linear increase in precipitation with time is obtained. The majority of the models project an increase of almost 20% by 2085 (period 2070-2100). This increase is expected due to the larger moisture content of the atmosphere in a warmer climate, combined with a projected strengthening of the westerly circulation in many models. It is known that a large part of the response of mean winter precipitation is governed by the lateral boundary conditions [Déqué et al. (2007)]. Approximately half of the RCM runs have been forced by either boundaries from ECHAM-r3 or HadCM3Q0. Thus, the spread in the RCM results is likely to under-sample the true uncertainty range since not all GCM boundary conditions are equally covered by the regional model ensemble.

For summer, changes in precipitation indicated by 25-75 percentile range are small until 2030. After 2030 decreases between between 10% to 30% towards the end of this century are predicted. As in winter, higher temperatures are expected to lead to higher atmospheric moisture contents, thus potentially leading to increases in rainfall. But in summer this is counteracted (partly over western Europe) by decreases in relative humidity. Projected changes in the atmospheric circulation with a larger influence of high pressure systems will also likely lead to a reduction of precipitation amounts. Progressive drying out of the soil over the continents could cause strong feedbacks on rainfall formation and even the atmospheric circulation. This could explain the non-linear trend in time of the precipitation. Some of the individual models (Appendix Figure A.2, models M1, M4, M17) indeed show a rapid decrease of mean precipitation after 2040-2060. Other model results do not show this behavior. We note that discontinuity in the trend in figure 2.2 is also partly due to the fact that the two models that project an increase in precipitation (M8 and M16) only ran up to 2050.

For autumn and spring, the medians of the model results show 5 to 10% increases. The increase however is not significant as approximately a third of the models actually predict a decrease.

The results for the individual models are shown in the Appendix (figure A.2). Except for a few models the trend in precipitation is reasonably uniform over the ensemble. However, the regional models driven by ARPEGE (M16 and M17) stand out. M17 shows almost no change for winter, but also projects a strong drying for spring and summer. M16 projects a decrease in winter and autumn precipitation, yet is together with M8 the only model that predicts increases in summer precipitation.

2.3 Year-to-year variability

Finally, we shortly comment on the year-to-year variability of the seasonal means (see figures A.3 and A.4 in the Appendix). As a measure of variability we used the standard deviation of the seasonal average. For all seasons, the variability in the ensemble is similar to the observations in the control period (1970-1999). However, because most models are too wet, the coefficient of variation (standard deviation divided by the mean) is underestimated. Considering climate change, the variability shows little change with time for all seasons except winter. We do find an increase in winter variability of approximately 20%, which can be attributed to a similar increase of total winter precipitation.

3 Coastal precipitation

3.1 Present-day climate

As mentioned in the introduction, we measure the coastal effect in precipitation by the difference between precipitation in the coastal area less than 50 km from the coastline with precipitation further inland (see Figure 1.2 for the coastal and inland area). We note the sign convention used here: a positive coastal effect refers to more precipitation in the coastal area compared to inland; negative to less precipitation in the coastal area. Thus, warm sea surface temperature are likely to cause an increase in the coastal effect, whereas cold temperatures are likely to cause a reduction of the coastal effect.

Each regional model simulation is given equal probability and the resulting distribution is plotted, and compared to the observations (figure 3.1). By this measure coastal effects in E-OBS are small in winter and summer. In spring coastal precipitation is approximately 0.2 mm day^{-1} (10% of the mean amount) less than inland, and in autumn approximately 0.3 mm day^{-1} (10-15%) more. Again, we would like to emphasize that the chosen measure is rather indiscriminative due to the broad coastal zone used and to the fact that we are considering seasons instead of separate months. For some months and closer to the coast precipitation differences could be substantially higher. For instance, precipitation amounts in October are in a small area near the coast approximately 40% higher than further inland (see figure 1.1).

The model ensemble is reasonably able to reproduce the size of the observed coastal effect in spring and autumn (figure 3.1). The ensemble median shows a good match with observations, but the model spread is also quite large. Thus, a considerable number of regional climate models produces results rather far from the observations (see also Appendix, figure A.5). Striking is that the three simulations with the UK Met-Office model (M1, M4, M6) have no coastal amplification of precipitation in autumn, but are rather close to the observations in spring. Results for the control period of the transient climate integration and the ERA40 driven integration are now more similar than for mean precipitation. In most models differences in coastal effect between these two simulations are small in spring, and moderate in autumn, and the differences appear to be largely unbiased. Thus, the results show that the lateral boundary condition used is of secondary importance, and has a smaller impact on the coastal effect of precipitation than on the mean precipitation over the Netherlands. This result also suggests that moderate differences in atmospheric circulation statistics, which primarily follow the flow conditions imposed at the lateral boundaries of the regional climate models, do not impact strongly on the coastal effect.

For winter and summer the observed coastal effect is close to zero. The model results show a large spread – larger than for spring and autumn – with a median of +0.1 mm day^{-1} in winter and -0.2 mm day^{-1} in summer. Thus the model ensemble is not well able to reproduce the observations. There are a few models that are close to the observations, but the majority is rather far off, in particular models M9 and M12 (see also Appendix, figure A.5 and figure A.6).

3.2 Climate change

The trend in the coastal effect is shown in figure 3.2. As in figure 2.2, we calculated 30-year moving averages with 10 year increments and show for each period the ensemble median and the ranges containing 50% and 100% of the models. The ensemble median shows an increase for all seasons: +0.05 for winter, +0.06 for

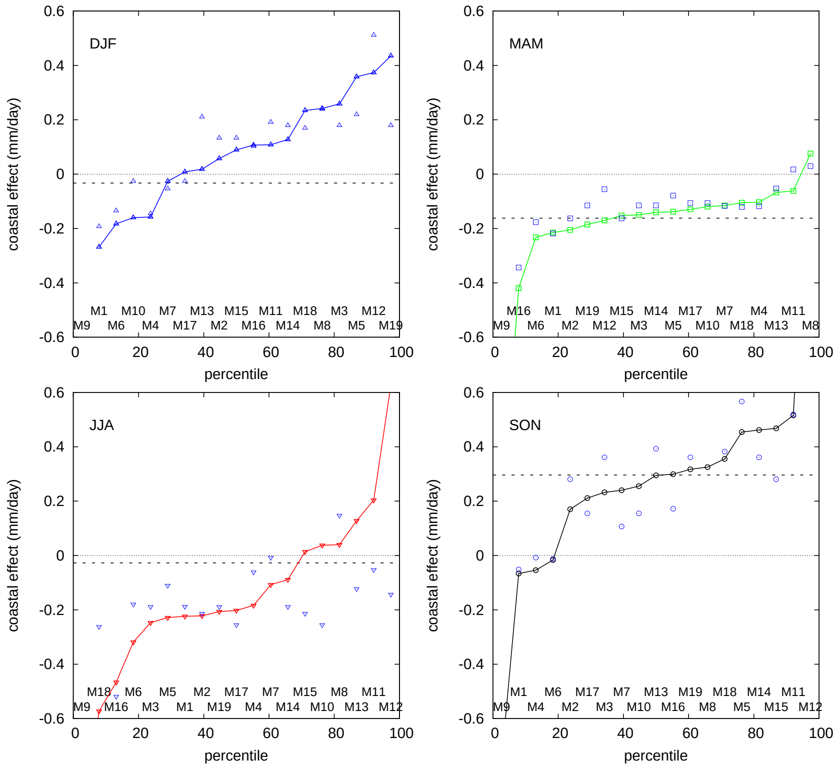

Figure 3.1: As figure 2.1, but now for the coastal effect for the period 1970-1999 in the model ensemble.

summer, +0.01 for autumn, and +0.02 mm day^{-1} for spring by the end of this century. Despite that the ensemble median of the predicted coastal effect is positive for all seasons, a considerable fraction of the models actually predicts a decrease. Only in winter, this fraction is below 25%, in the other seasons it is larger than 25% (but smaller than 50%).

The observed trend derived from E-OBS is generally within the spread of the model ensemble, except for the summer period. For summer the increase in coastal effect over the last 50 years appears to surpass the envelope of the RCM predictions. We note that divergence of the model results around the reference year 1985 (period 1970-2000) is not necessarily a trend, but is more likely to be due to natural variability. The upward trend in summer in coastal precipitation with respect to inland is consistent with earlier findings [Lenderink et al. (2009)].

The results for the individual models (Appendix, Figure A.6) clearly reveals considerable variations from one 30-year time period to the other. There are a few models (M3, M12, M16) that produce very large variations, which appear outside the range of the variations produced by the other models. It was already noted that the integration with M12 is suspect due to the large difference between the coastal effect in the transient simulation and the ERA40 driven simulation.

Since the coastal effect in precipitation is forced by sea surface temperatures, and the differences between the temperatures at sea and above land, we continue to look at the trends in the sea surface temperature. Trends in sea surface temperature are plotted in Figure 3.3. The sea surface temperature is the average over the dark blue area in Figure 1.2. On average, the temperature rises approximately 2 degrees by the end of this century. There are a number of simulations that give rather strange results, in particular for the integration that run only until 2050. This is visible in the

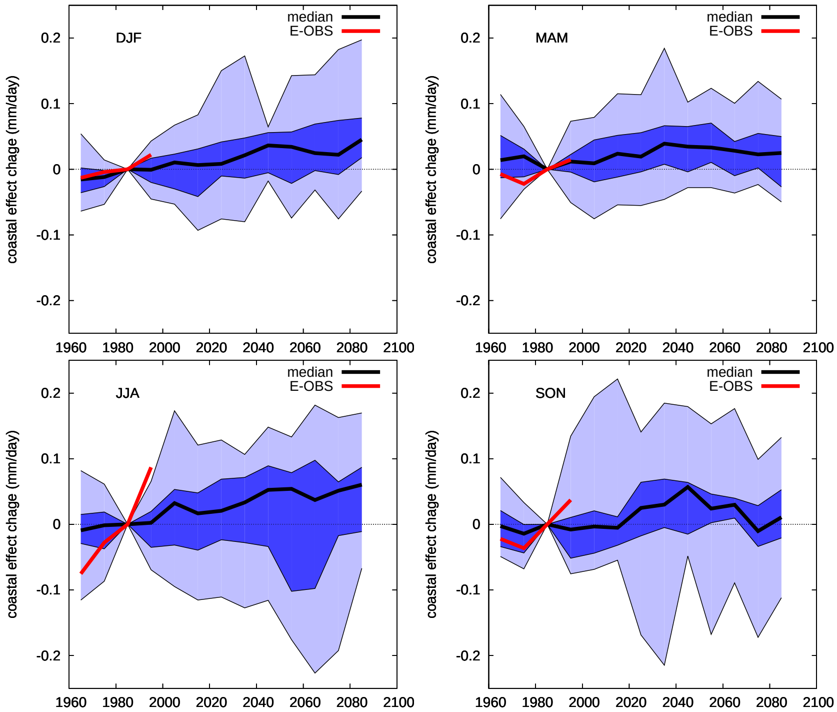

Figure 3.2: As figure 2.2, but now for the trends in the coastal effect relative to the period 1970-1999.

graphs in the discontinuity after 2035 (2020-2050; that is, last period covered in these shorter integrations). The evolution of the individual models (Appendix, figure A.8) shows that two models display very strong variations in the sea surface temperature, even with decreasing sea surface temperature in summer. These models (M3 and M16) are the same as those that produce the large variations in coastal effect as noted before.

On average, the rise in sea surface temperature is quite low in these integration. The rise of the temperature above land is approximately 0.5-1.0 degree higher. One of the reasons that the temperature rise is quite limited could be due to the fact that the global models hardly resolve the North Sea. The lag of temperature increase of the North Sea (compared to land) could well mean the increase in coastal effect is underestimated in these runs.

3.3 Correlation with North Sea temperature

In this section we investigate how the coastal effect relates to North Sea temperatures. For this purpose we fitted a linear relation between the coastal effect and sea surface temperature using least square fitting. This is done for 30-year averages and 1-year averages. The 30-year averages are advanced 10 years in time, thus giving 13 data points. Results are shown in figure 3.4, in which 30-year averages are the big black symbols and 1-year averages are smaller colored symbols. The single season averages are quite noisy but the correlations based on 1-year and 30-year averages are comparable as soon the spread in temperature and precipitation is large enough. We note that for some seasons and models the temperature rise over the 21st century is quite small, so that the spread in yearly average values is much larger than the temperature rise over the whole period. In that case, variability on the yearly time scale dominates the climate change signal. As mentioned before the small rise in North Sea temperature appears not trustworthy.

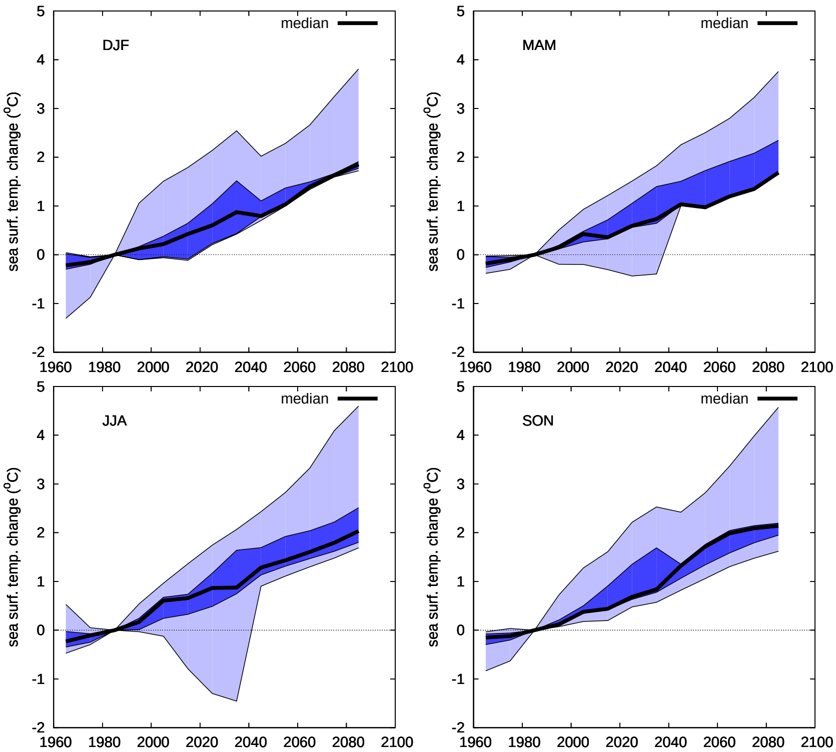

Figure 3.3: As figure 2.2, but now for the trend in sea surface temperature. We note that the far majority of the regional models use boundaries from either HadCM3Q0 or ECHAM-r3, which results in a rather skewed distribution of the change in sea surface temperature. Consequently for some seasons the median change is almost equal to the minimum change in the model ensemble. Note also the fact that after 2050 only 13 regional model simulations are left, which causes the jump in the minimum value for spring and summer around 2040.

The plotted 30-year averages contain overlapping time periods, and only 4 points are independent. In the following we will use the results from the fitting to the averages over one season. The regression coefficient of dependency of the coastal effect on SSTs is shown in figure 3.5. The ensemble mean shows in all seasons a small positive dependency of the coastal effect on SST. The largest effect is in summer and winter, whereas the effect in spring is smaller. In autumn it is close to zero.

Secondly, the dotted lines in figure 3.5 indicate the median change in precipitation from figure 3.2 divided by a 2° increase in SST in 2100. A two degrees temperature rise is representative of the far majority of the RCM integrations. In summer, the climate change response in coastal effect is consistent with the regression coefficients derived here from the interannual variability. This is a strong indication that the changing SSTs are related to the change in coastal effect. In winter, the regression coefficients are larger than the dependency derived from the response in coastal effect due to climate change. In autumn and spring, the regression coefficient is consistent with the climate change response, but the average signal is quite small.

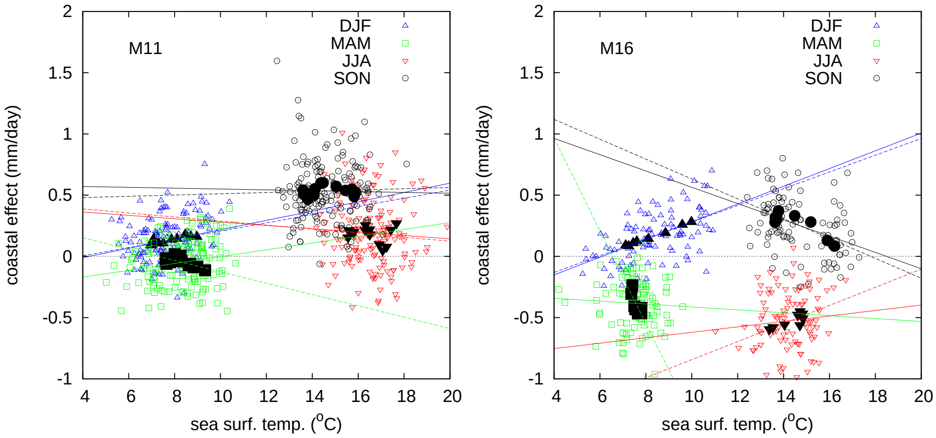

Figure 3.4: Scatter plot of the coastal effect (y-axis, in mm day^{-1}) and North Sea temperature (x-axis, in $^\circ$C) for model M11 (left) and M16 (right). Colored symbols are single seasons, whereas the black symbols are 30-year averages. Dotted (solid) lines are fits to the 30 (1) year seasonal averages.

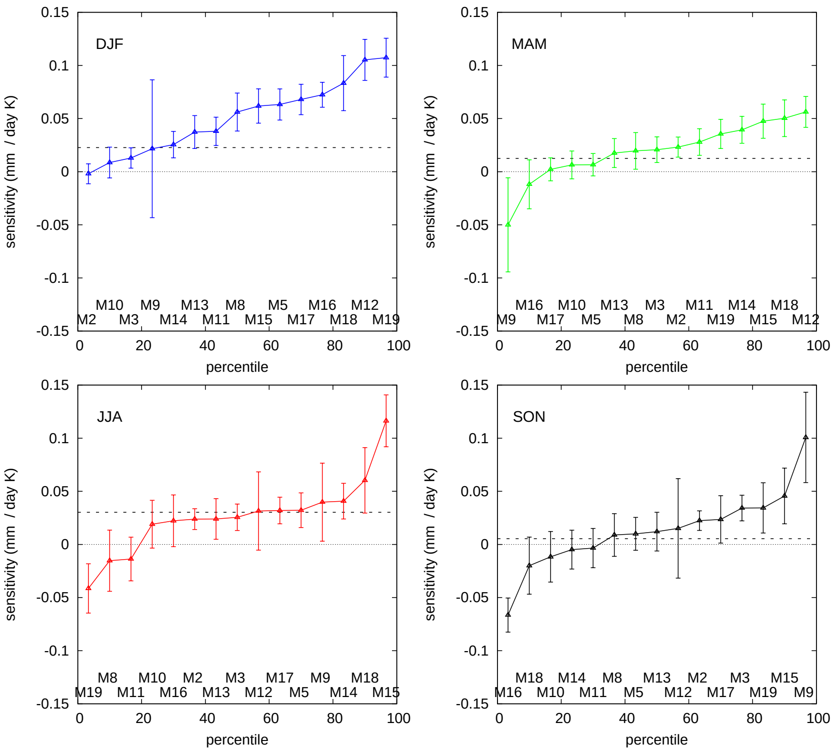

Figure 3.5: Sensitivity of coastal effect (in mm day^{-1} K^{-1}) to the sea surface temperature based on averages over single seasons. For reference, the dotted horizontal lines indicate the median change in coastal effect by 2100 from the model ensemble divided by the median, 2 $^\circ$C increase in SST. Vertical bars indicate standard error for the fit for each model.

4 Summary and conclusions

We investigated the climate response in a large ensemble of 19 regional climate model integrations. These runs have been performed in the European project ENSEMBLES, and were run at a (at that time) unprecedented high resolution of 25 km and simulation length of 100 to 150 years. From the 19 model simulations only 13 covered the complete period 1950 to 2100, the others ran up to 2050 only. These long, transient regional climate model integrations have been forced at their lateral boundaries by output from a number of global climate models. We focused on the mean response in precipitation and the change in precipitation patterns within the Netherlands. For the latter we studied the coastal effect in precipitation, which we defined as the difference between precipitation amounts closer than 50 km from the coastline and precipitation amounts further inland. In ENSEMBLES also integrations for all regional climate models using ERA40 re-analysis boundaries have been performed. This enables us to investigate the performance of the regional climate models under flow conditions that are controlled to be close to reality.

Comparing the model results of the long, transient integrations for the control period (1970-2000) with the observations, it shows that the regional models have in general a positive bias in mean precipitation for the Netherlands. In winter, this bias is quite significant. The integrations with the re-analysis boundaries show that about half of the bias can be explained by biases in the large scale forcing from the GCM. In summer and autumn the spread in the model results is quite large, and there are models that show a negative bias. Again, it is shown that much of the spread is related to the GCM boundaries.

For the different seasons, the mean precipitation change is consistent with the Dutch KNMI'06 climate scenarios. In winter precipitation increases by approximately 20%, whereas in summer an equal decrease is projected by the model ensemble. In spring and autumn mean precipitation changes are small, yet on average positive.

The coastal effect is reasonably captured in the model simulations in spring and autumn. The model results scatter around -0.2 mm day^{-1} in spring and 0.3 mm day^{-1} in autumn. This is about 10-15% of the total precipitation occurring in spring and autumn. In winter and summer the model results show a very large spread, with on average a positive bias in winter and a negative bias in summer. In contrast to the mean precipitation, the bias is almost independent of the boundaries used; results from the integrations using ERA40 re-analysis data are similar to those from the transient model integrations. Finally, we note that a few of the model integrations produce results that are very far from the observations, and therefore these simulations appear erroneous.

On average, the coastal effect increases in the transient regional climate model simulations. Thus coastal precipitation is expected to increase compared to precipitation inland. However, the increase is quite small with the median of the model results projecting by the end of this century increases of 0.01 mm day^{-1} in autumn, 0.02 mm day^{-1} in spring, 0.05 mm day^{-1} in winter and 0.06 mm day^{-1} in summer. The spread in the ensemble (uncertainty) is also quite large; of the 13 model integrations running up to 2100, actually 2 in winter, 3 in summer and spring, and 4 in autumn project a decrease in coastal effect at the end of the integration period. A regression of the coastal effect on sea surface temperatures shows similar numbers if we assume a temperature rise of 2 degrees of the North Sea, which is approximately the median response of the sea surface temperatures in the model ensemble. In winter, the regression suggest a slightly higher dependency of the coastal effect on sea surface temperature. Despite that in absolute terms the changes in coastal effect over the century are quite small, in relative terms compared to the coastal effect in the present-day climate of order 0.2 mm day^{-1} they are not negligible, amounting up to 20-30% of this value.

Finally, we would like to address the limitations of establishing changes in the coastal effect from the present model results. First, the resolution of 25 km is still relatively low compared to the features of interest. Due to this we had to take a rather broad coastal region of 50 km, which results in a rather small coastal effect of 10-15% of the mean precipitation. In the observations and for some months the coastal effect can be much larger. Second, the prescribed sea surface temperatures in the regional climate model simulations are a limitation because they are derived directly from the coarse resolution GCM simulations. Since the North Sea is hardly resolved in the global models, the realism of these temperatures are limited and the temperature rise of the North Sea may well be underestimated. Even more, some of the regional model simulations appear to have rather unrealistic North Sea temperatures in which the temperature hardly rises in some seasons or show very large interdecadal variations. Third, a general limitation of these models is their ability to model convective processes in the atmosphere. Convection plays an essential role in showers, and the lifecycle of showers – their initiation, growth, and advection – plays a crucial role in determining the coastal effect. The present generation of climate models does not resolve convection, but uses parameterizations instead. Parameterizations consist of relatively simple rules expressing the effect of convection in terms of the model mean over the grid boxes. This could, for instance, result in model errors in advecting showers from sea to the land [Lenderink et al. (2009)].

As an outlook, we continue this research with a higher resolution version of RACMO2 at 12 km resolution. In addition, a more realistic description of North Sea temperature is obtained from building in a simple slab ocean model into RACMO2. This slab model provides a more realistic coupling between the course resolution SSTs from the global model and the atmosphere in RACMO2. Finally, this system will be evaluated more carefully against the observations, with particular emphasis on the representation of the coastal effect and possible errors and biases resulting from the model representation of convection.

Acknowledgements. We acknowledge the E-OBS dataset from the EU-FP6 project ENSEMBLES (http://www.ensembles-eu.org) and the data providers in the ECA&D project (http://eca.knmi.nl). NOAA OI SST V2 data provided by the NOAA/OAR/ESRL PSD, Boulder, Colorado, USA, from their Web site at http://www.esrl.noaa.gov/psd/. Janette Bessembinder is acknowledged for careful proofreading. This research has been financed by the Dutch project Knowledge for Climate (KfC) (project KKF 1a).

A Plots with the results of the separate regional climate model simulations

Here, we present plots for the separate ensemble members. Lines and symbols for the different models can be found in table 1.1.

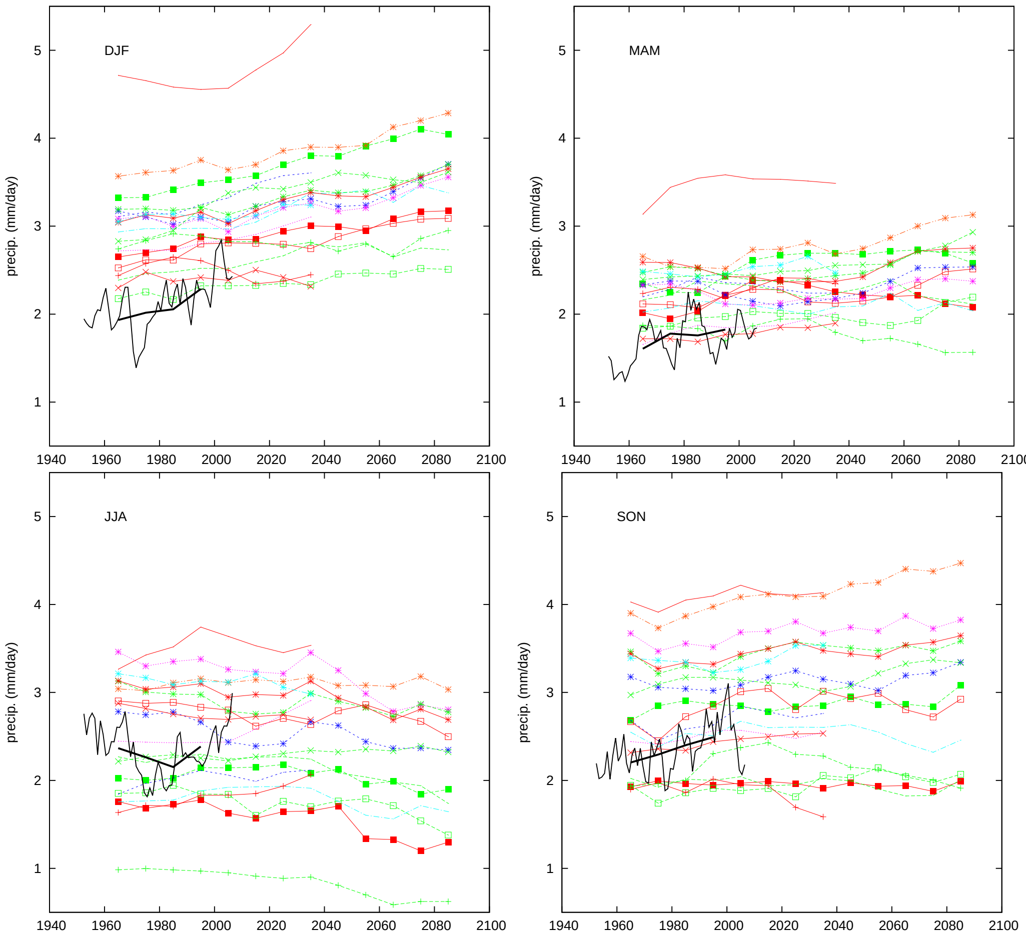

Figure A.1: 30-year seasonal average of the mean precipitation over the Netherlands. A five-year (thin black line) and a 30-year (thick black line) average of the E-OBS dataset are added for comparison.

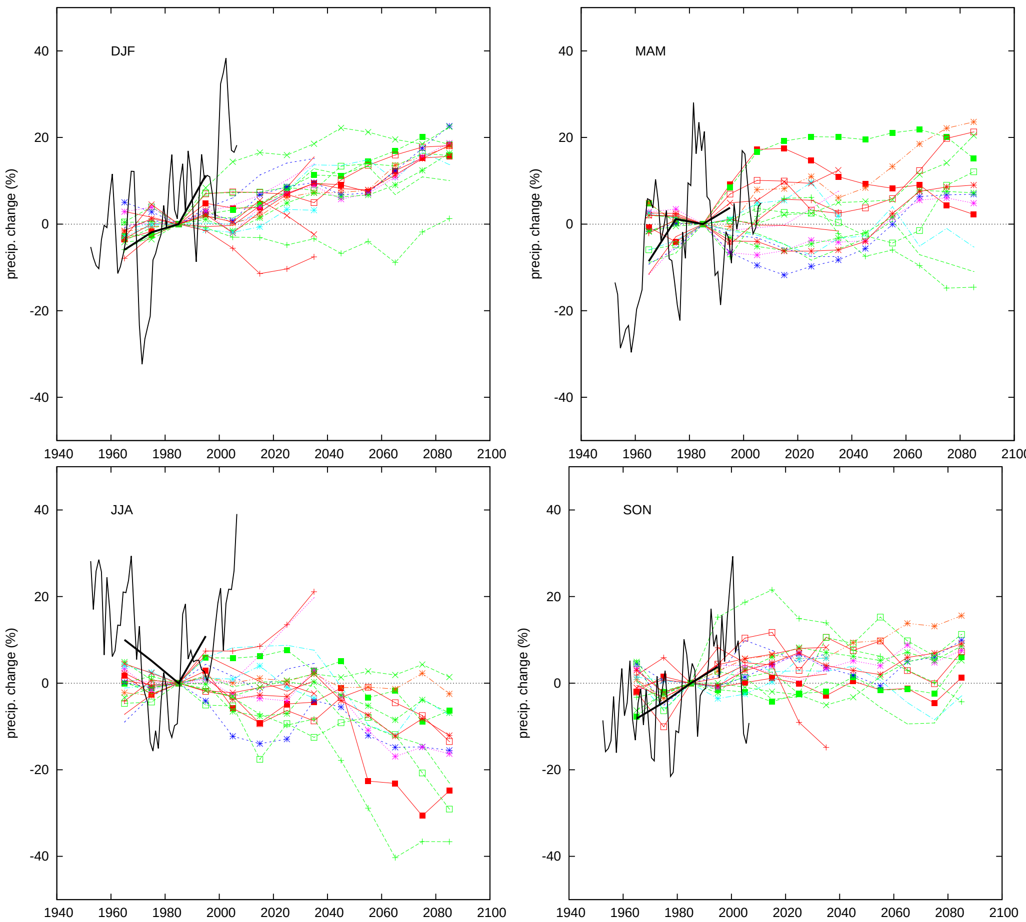

Figure A.2: 30-year seasonal average of the precipitation over the Netherlands, relative to the period 1970-1999. A five-year (thin black line) and a 30-year (thick black line) average, both relative to 1970-1999, of the E-OBS dataset are added for comparison.

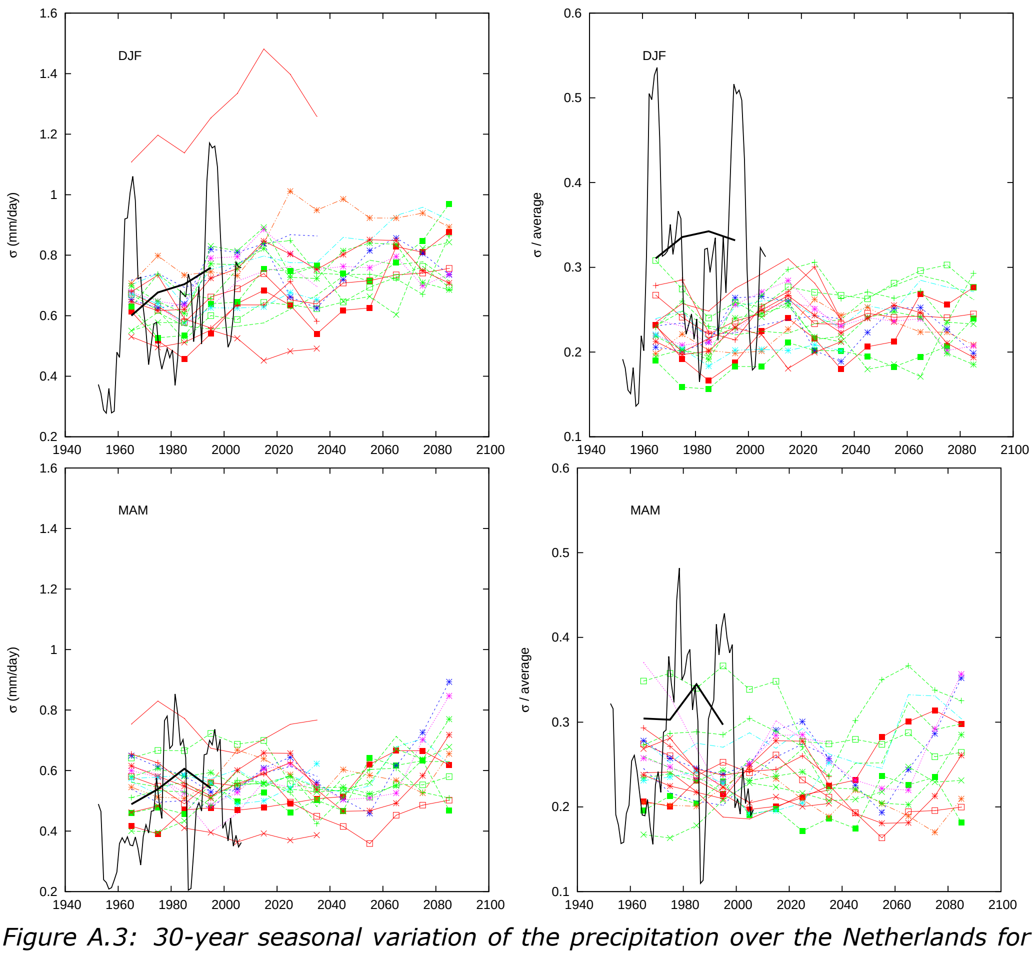

Figure A.3: 30-year seasonal variation of the precipitation over the Netherlands for winter and spring. In absolute precipitation (left) and relative to the average (right). A five-year (thin black line) and a 30-year (thick black line) average of the E-OBS dataset are added for comparison.

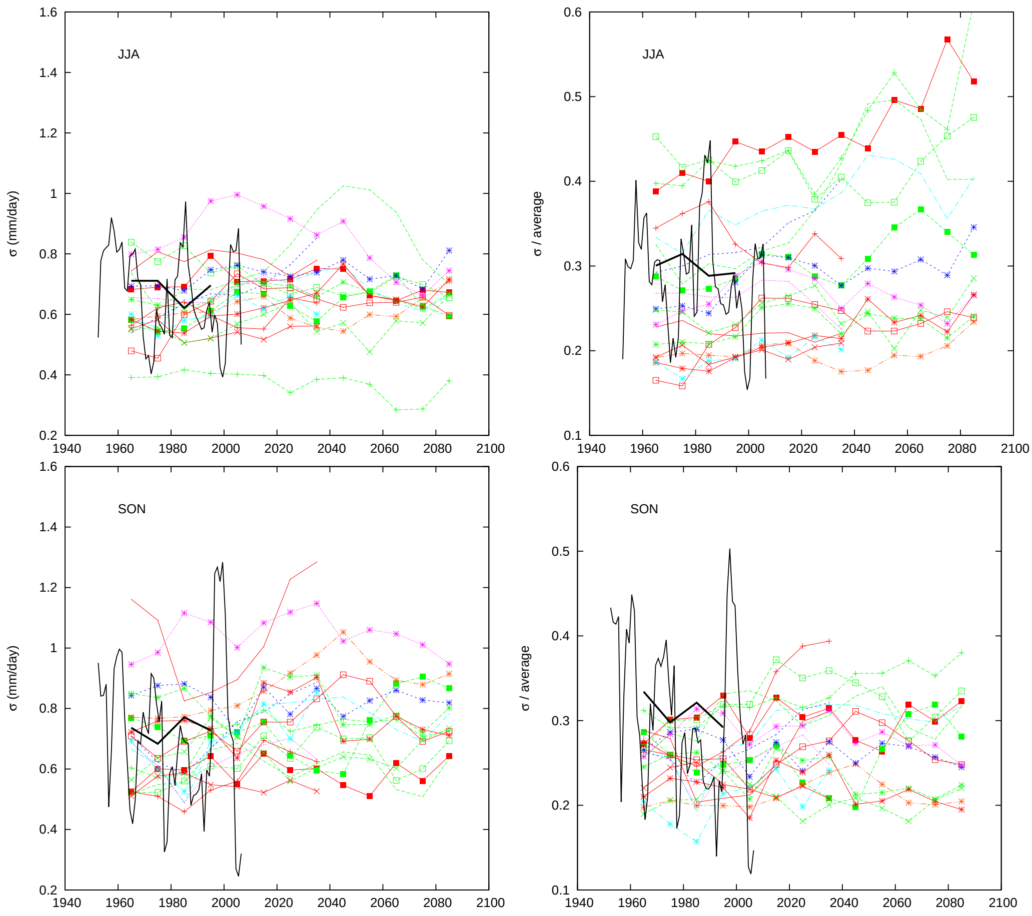

Figure A.4: As figure A.3, but now for summer and autumn.

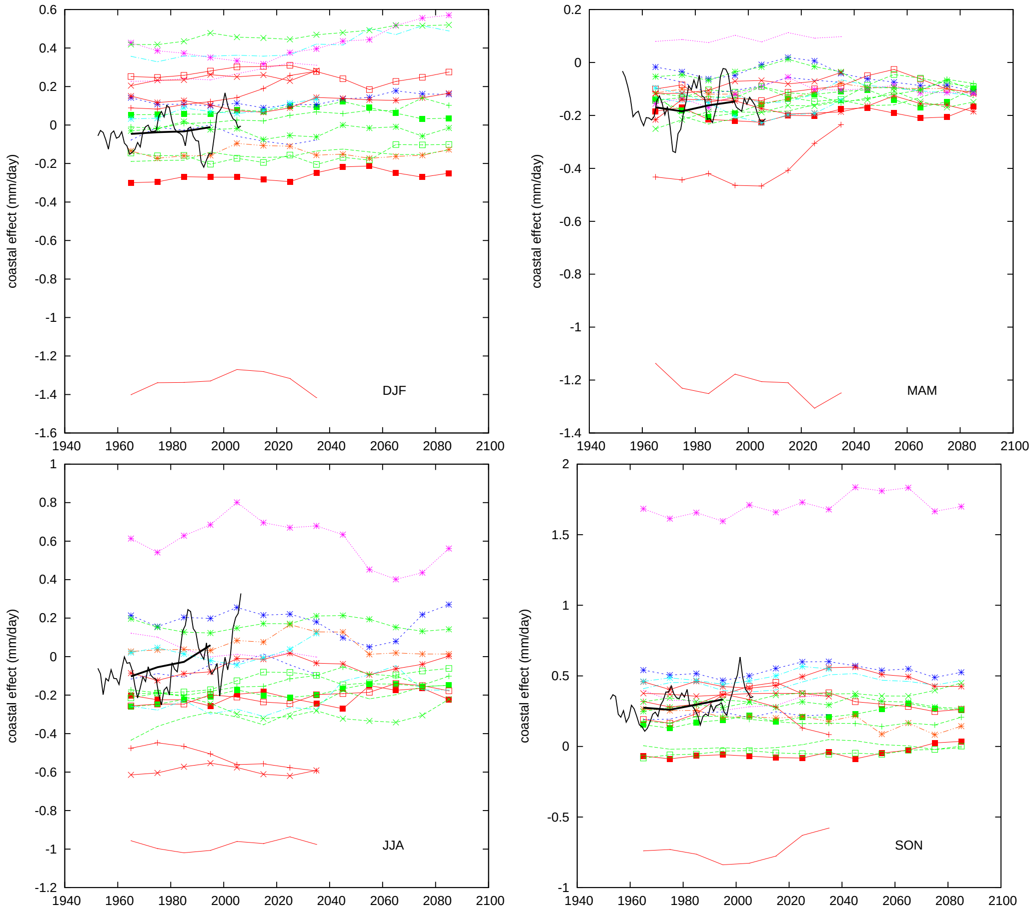

Figure A.5: 30-year seasonal average of the coastal effect in precipitation for the Netherlands. A five-year (thin black line) and a 30-year (thick black line) average of the E-OBS dataset are added for comparison.

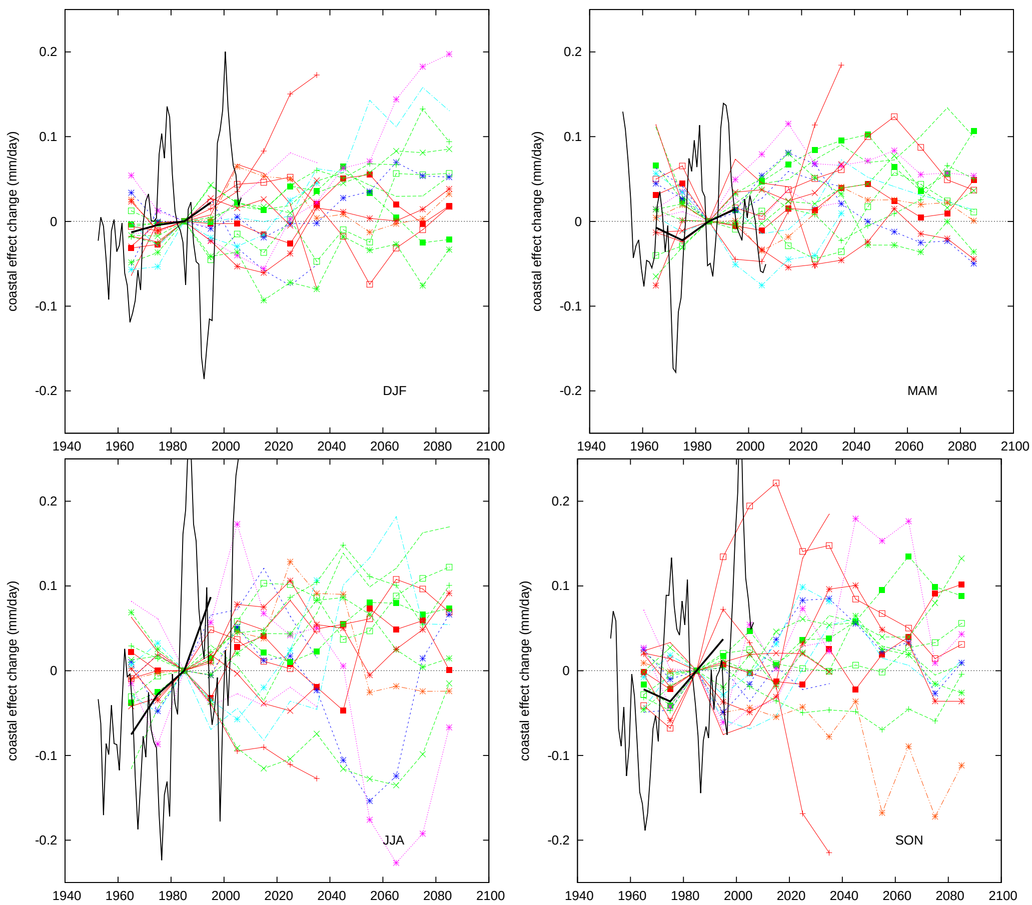

Figure A.6: 30-year seasonal average of the coastal effect in precipitation for the Netherlands, relative to the control period 1970-1999. A five-year (thin black line) and a 30-year (thick black line) average of the E-OBS dataset are added for comparison.

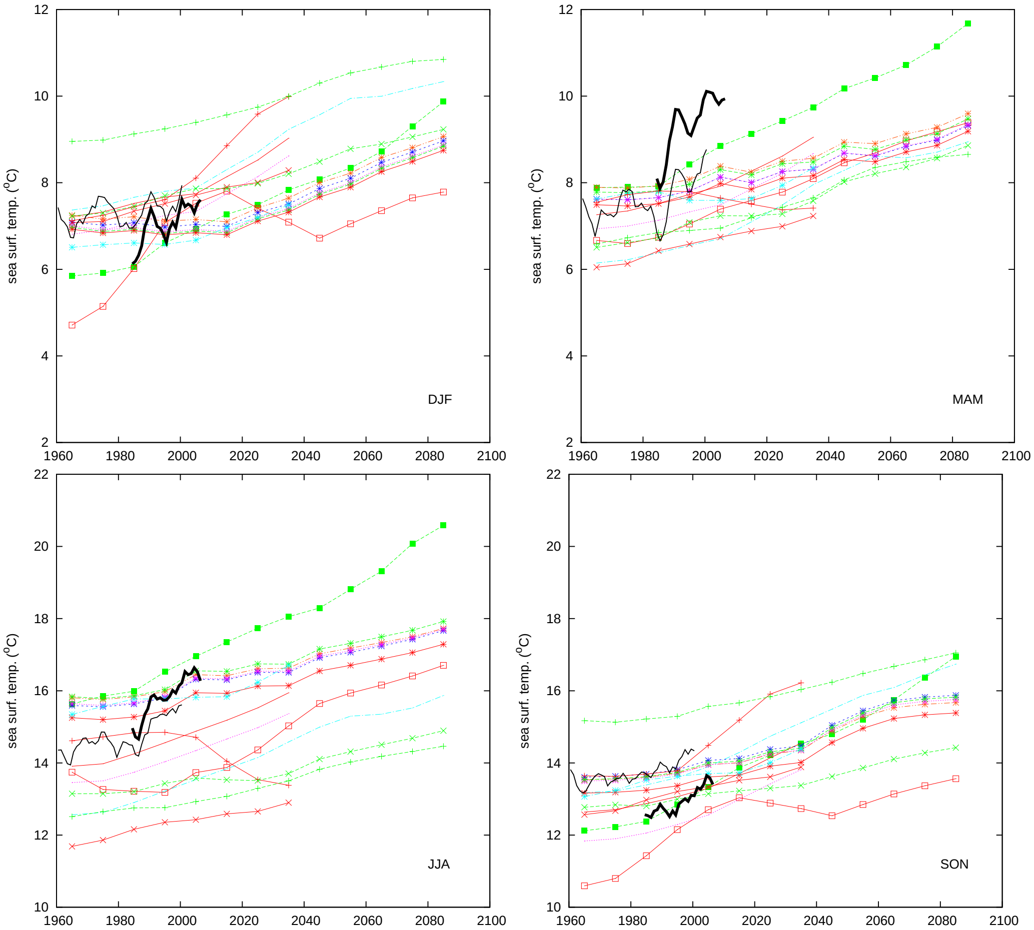

Figure A.7: 30-year seasonal average of the sea surface temperature for the North Sea. A five-year average of OIv2 (thick black line) and RACMO2 ERA-40 (thin black line) are added for comparison.

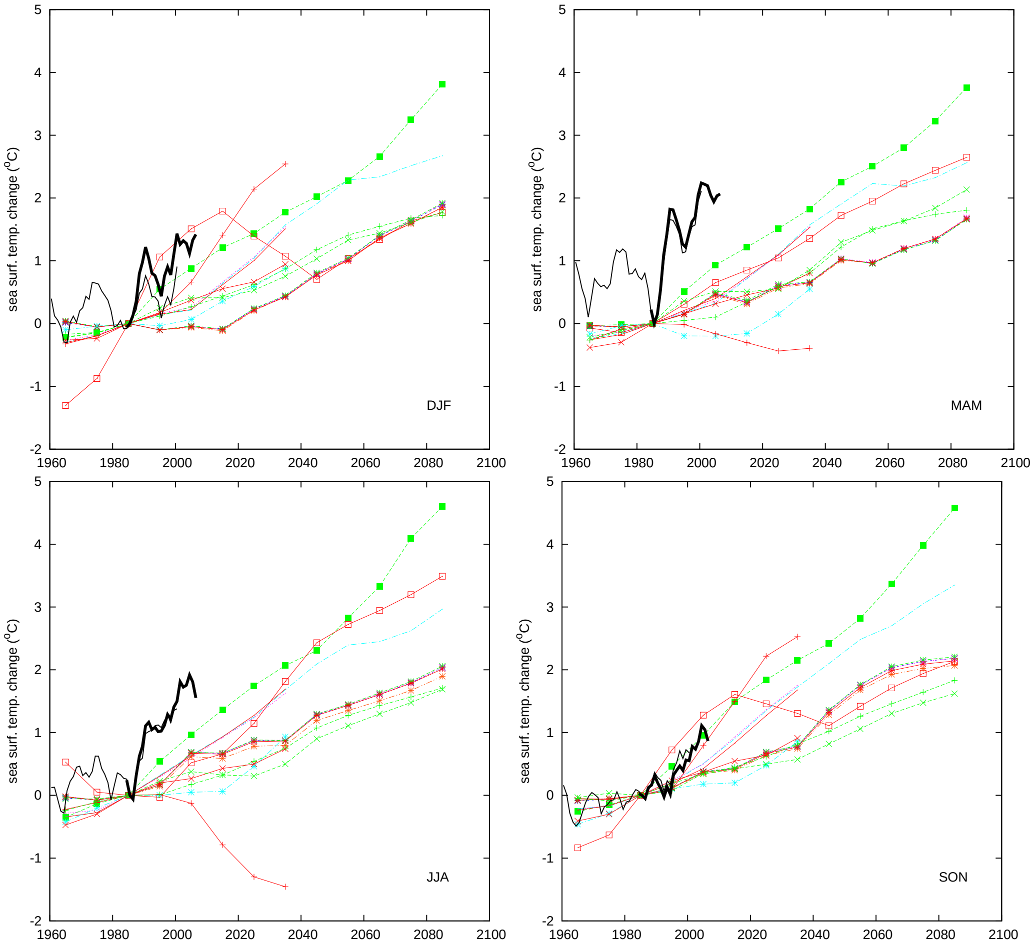

Figure A.8: 30-year seasonal average of the sea surface temperature for the North Sea, relative to the period 1970-1999. A five-year average of OIv2 (thick black line) and RACMO2 ERA-40 (thin black line) relative to 1983-1987 are added for comparison.

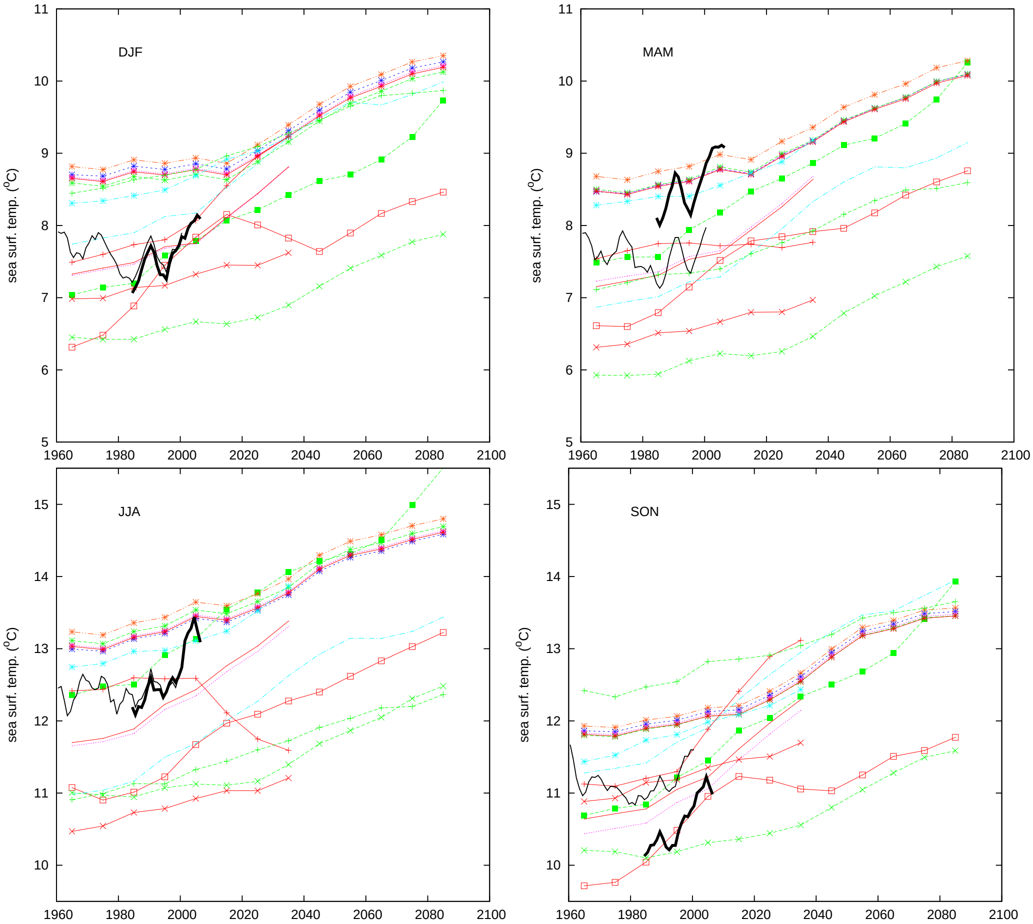

Figure A.9: 30-year seasonal average of the sea surface temperature for a larger sea area between -10 to 10 East and 50 to 65 North. A five-year average of OIv2 (thick black line) and RACMO2 ERA-40 (thin black line) are added for comparison.

References

Déqué, M., Rowell, D., Lüthi, D., Giorgi, F., Christensen, J. H., Rockel, B., Jacob, D., Kjellström, E., de Castro, M., and van den Hurk, B. (2007). An intercomparison of regional climate simulations for europe: assessing uncertainties in model projections. *Climate Change*, 81:53–70.

Haylock, M. R., Hofstra, N., Klein Tank, A. M. G., Klok, E. J., Jones, P. D., and New, M. (2008). A european daily high-resolution gridded data set of surface temperature and precipitation for 1950-2006. *J. Geophys. Res.*, 113:D20119.

Held, I. M. and Soden, B. J. (2006). Robust responses of the hydrological cycle to global warming. *J. Climate*, 19:5686–5699.

Hewitt, C. and Griggs, D. (2004). Ensembles-based predictions of climate changes and their impacts (ENSEMBLES). *EOS*, 85:566.

Lenderink, G., van Meijgaard, E., and Selten, F. (2009). Intense coastal rainfall in the Netherlands in response to high sea water temperatures: analysis of the event of august 2006 from the perspective of a changing climate. *Climate Dynamics*, 32:19–33.

Lenderink, G., van Ulden, A., van den Hurk, B., and Keller, F. (2007). A study on combining global and regional climate model results for generating climate scenarios of temperature and precipitation for the Netherlands. *Climate Dynamics*, 29(2):157–176.

O'Gorman, P. A. and Muller, C. J. (2010). How closely do changes in surface and column water vapor follow clausius-clapeyron scaling in climate change simulations? *Environmental Research Letters*, 5(2):025207.

Reynolds, R. W., Rayner, N. A., Smith, T. M., Stokes, D. C., and Wang, W. (2002). An improved in situ and satellite sst analysis for climate. *Journal of Climate*, 15(13):1609–1625.

Uppala, S., Kallberg, P., Simons, A., and 43 co-authors (2005). The ERA-40 re-analysis. *Quart. J. Roy. Meteor. Soc.*, 131:2961–3012.

van den Hurk, B., Bessembinder, J., Burgers, G., and Co-Authors (2006). Knmi climate change scenarios 2006 for the Netherlands. Technical Report WR-2006-01, Royal Netherlands Meteorological Institute.

A complete list of all KNMI-publications (1854 – present) can be found on our website

www.knmi.nl/knmi-library/knmipub_en.html

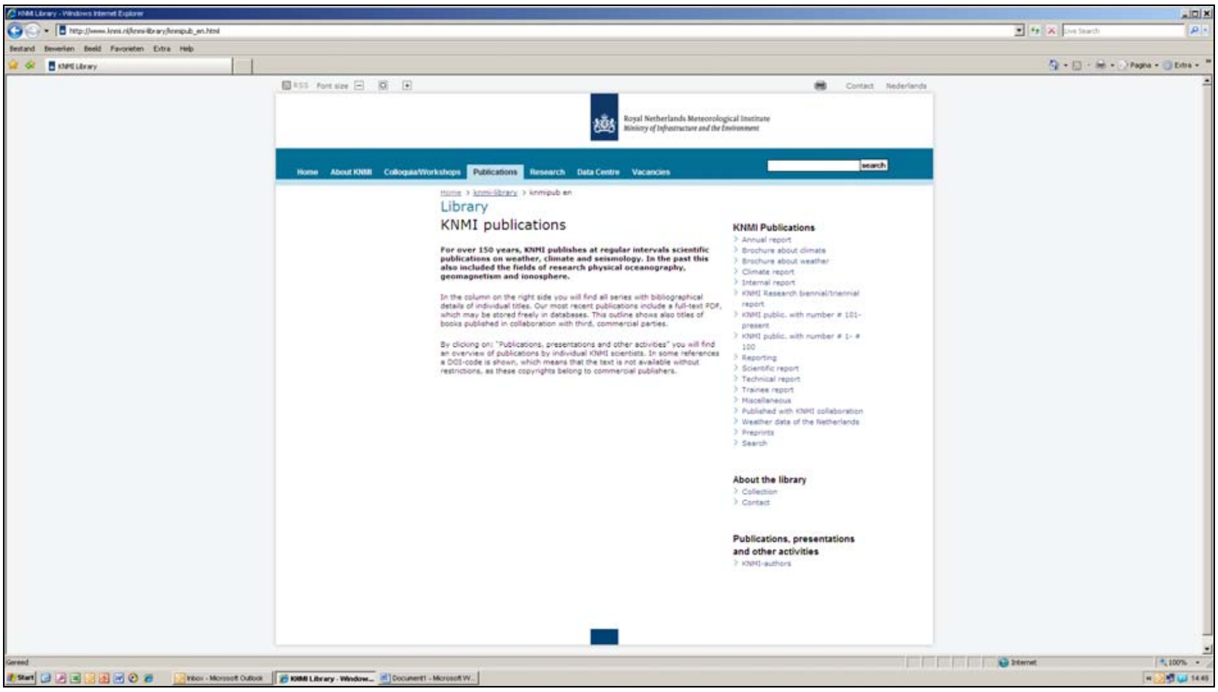

The most recent reports are available as a PDF on this site.